

Supporting Information

Highly efficient white organic light-emitting diodes based on balanced bipolar-transporting blue hybridized local charge transfer fluorophore

Tengyue Li,^a Shian Ying,^a Huayi Zhou,^a Runze Wang,^a Chenglin Ma,^a Mizhen Sun,^a

Mingliang Xie,^a Qikun Sun,^a Wenjun Yang,^a Shanfeng Xue^{a*}

^a Key Laboratory of Rubber-Plastics of the Ministry of Education, School of Polymer Science & Engineering, Qingdao University of Science and Technology, 53-Zhengzhou Road, Qingdao 266042, P. R. China.

*Corresponding author. E-mail: sfxue@qust.edu.cn;

S1 Materials and Measurements

S1.1 Materials

The small molecule *N, N*-diphenyl-4-(7-(4-(5-phenyl-1,3,4-oxadiazol-2-yl) phenyl)9,9-dipropyl-9-*H*-fluoren-2-yl) aniline (TPACFOXZ) as the emitting material and dopant host was synthesized in our laboratory.¹ ITO is indium tin oxide used as an anode. PEDOT: PSS is Poly(2,3-dihydrothieno-1,4-dioxin)-poly(styrenesulfonate) used as a hole injection layer. TCTA is 4,4',4''-Tris(carbazol-9-yl)triphenylamine. PO-01 is Bis(4-phenyl-thieno[3,2-*c*] pyridinato-C2, N) (acetylacetonato)iridium (III) used as a yellow phosphorescent dopant in the luminescent layer. TPBi is 1,3,5-Tris(1-phenyl-1-*H*-benzimidazol-2-yl) benzene used as the electron transport layer. LiF is lithium fluoride used as an electron injection buffer layer. All these materials were used from commercial purchases without further purification.

S1.2 Instrumentation and Device Fabrication:

ITO-coated glass with a sheet resistance of 15–20 Ω per square was used as the substrate, then cleaned sequentially in an ultrasonic bath with acetone, detergent, deionized water and isopropanol, and finally dried in an oven at 120°C for 1 hour. After oxygen plasma cleaning at 20 Pa under pure oxygen pressure for 7 minutes, a 40 nm thick PEDOT: PSS layer was first spin-coated from aqueous solution onto the ITO substrate, then held at 145°C for 25 minutes, and slowly cooled for thermal annealing. Subsequently, the treated substrate was put into the vacuum vapor deposition bin, and after the air pressure was lower than 1.6×10^{-4} Pa, the baffle of organic element TCTA and heating function were opened, TCTA was vaporized and the vaporization rate was

adjusted to 0.1 nm/s, then the TCTA was closed after vaporization of 20 nm. Heating and baffle. Put TPACFOXZ and PO-01 under the same frequency meter detection, open the baffle of TPACFOXZ and PO-01 at the same time to adjust its evaporation rate ratio to 8%, then open the substrate to start evaporation, keep the evaporation rate at 0.1 nm/s, and close the heating and baffle after evaporation of 10 nm. Turn on the heating function of the organic element TPBi, evaporate TPBi, adjust the evaporation rate to 0.1 nm/s, then turn on the substrate baffle and start evaporation, turn off the heating and baffle of TPBi after evaporation of 30 nm. Turn on the baffle and heating function of the metal element, vaporize LiF, adjust the vaporization rate to 0.02 nm/s, and turn off the TCTA heating and baffle after vaporizing 1 nm. Turn on the baffle and heating function of metal element Al, vaporize metal Al, adjust the vaporization rate to 0.5 nm/s, then open the baffle to vaporize 10 nm for purification, and turn off the Al heating and baffle after vaporizing 100 nm.

The current–voltage–brightness characteristics were measured by using a Keithley source measurement unit (Keithley 2450 and LS-160), EL spectra were measured with 14 Flame-S (Serial Number: FLMS16791, Range: >350 nm). EQEs were calculated from the luminance, current density, and EL spectrum, all the results were measured in the forward viewing direction without using any light out-coupling technique. According to equation following (Formula S1).

$$EQE = \frac{\pi \cdot L \cdot e}{683 \cdot I \cdot h \cdot c} \cdot \frac{\int_{380}^{780} I(\lambda) \cdot \lambda \cdot d\lambda}{\int_{380}^{780} I(\lambda) \cdot K(\lambda) \cdot d\lambda} \quad (1)$$

where L (cd/m^2) is the total luminance of device, I (A) is the current flowing into the EL device, λ (nm) is EL wavelength, $I(\lambda)$ is the relative EL intensity at each wavelength and obtained by measuring the EL spectrum, $K(\lambda)$ is the Commission International de L'Eclairage chromaticity (CIE) standard photopic efficiency function, e is the charge of an electron, h is the Planck's constant, c is the velocity of light. The efficiency roll-offs of blue OLED device were calculated from maximum EQE and the EQE at luminescence of 1000 cd/m^2 . According to equation following (Formula S2):

$$\eta = \frac{EQE_{\max} - EQE_{1000}}{EQE_{\max}} \quad (2)$$

S2 Supplementary figures and tables

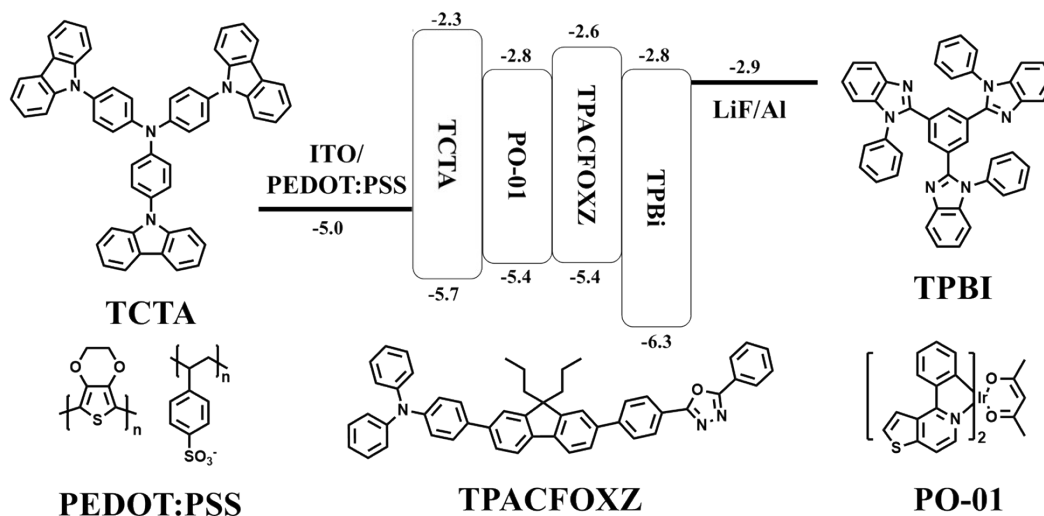


Fig S1. HOMO/LUMO energy levels and molecular structure used in the devices.

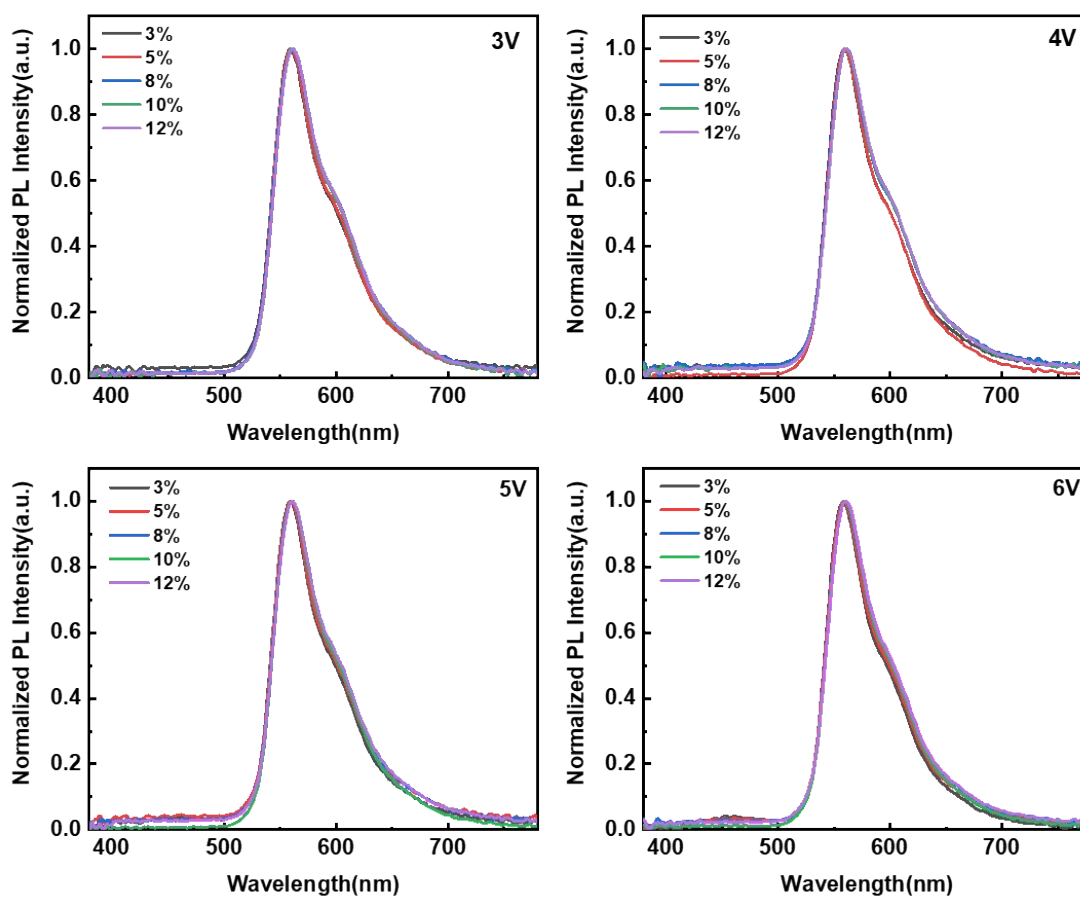


Fig S2. Electroluminescence spectra of yellow OLEDs with different voltages.

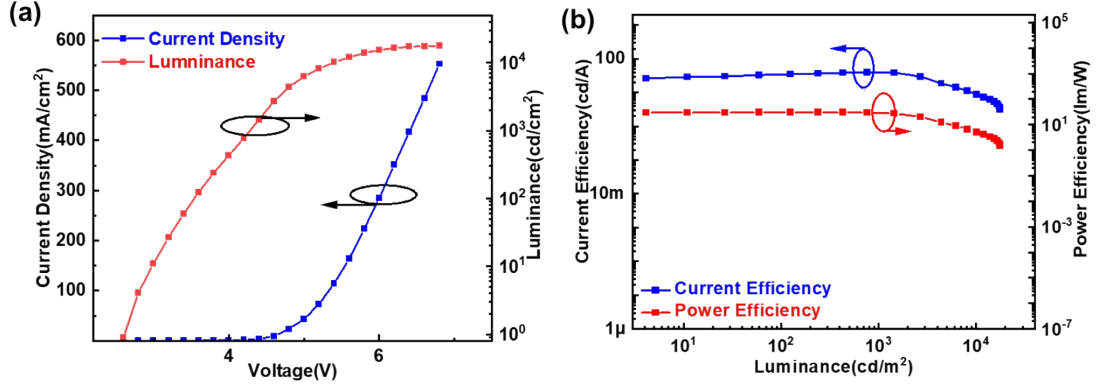


Fig S3. (a) Current density-voltage-luminance curves. (b) Current efficiency-luminance-power efficiency curves of the device **W**.

	$\frac{\text{EQE}^{(a)}}{\text{Max}}$ [%]	$\text{EQE}_{@1000}$ [%]	$\text{CE}_{\text{max}}^{(c)}$ [cd/A]	$\text{PE}_{\text{max}}^{(d)}$ [lm/W]	$\text{CIE}_{1000}^{(e)}$	$\text{L}_{\text{max}}^{(f)}$ [cd/m ²]	Ref.
TPACFOXZ	27.1	23.8	78.8	53.8	(0.35, 0.39)	32453	This work
2TPA-PPI	25.4	25.2	—	71.0	(0.50, 0.40)	—	2
mCP-BP-DMAC	20.6	18.6	45.7	50.5	(0.46, 0.43)	47320	3
DCB-BP-DMAC	22.1	20.1	44.7	50.8	(0.54, 0.41)	53900	3
28-DMAC-DPS	22.7	20.0	65.9	78.1	(0.30, 0.44)	28325	4
26-DMAC-DPS	21.4	18.1	60.2	70.2	(0.31, 0.46)	45520	4
TPE-TADC	19.2	19.1	56.7	55.2	(0.44, 0.46)	49002	5
piq-DCB-BP-SFAC	17.8	10.1	31.2	28.3	(0.33, 0.39)	8479	6
TPA-aq-DCB-BP-SFAC	19.1	7.4	47.1	46.2	(0.48, 0.46)	11750	6
PIPD-MP-DPA(2)	21.6	17.7	71.1	57.2	(0.45, 0.49)	45000	7
PIPD-MP-DPA(4)	16.3	13.8	45.5	38.3	(0.42, 0.48)	48320	7
2M-ph-3CzAnBzt	21.5	20.8	—	—	(0.47, 0.50)	—	8
SSFAPO	25.1	—	77.6	82.6	(0.42, 0.50)	—	9
DSFAPO	20.1	—	63.3	69.7	—	—	9
TSFAPO	15.9	—	49.4	51.7	—	—	9

Table S1. The summary of roll-off at 1000 cd/m² and Maximum EQE in WOLEDs.

^(a) $\text{EQE}_{\text{Max}/1000}$: EQE of maximum/at 1000 cd/m². ^(c) CE_{max} : Maximum current efficiency. ^(d) PE_{max} : Maximum power efficiency. ^(e) CIE coordinates at 10000 cd/m². ^(f) L_{max} : Maximum luminance.

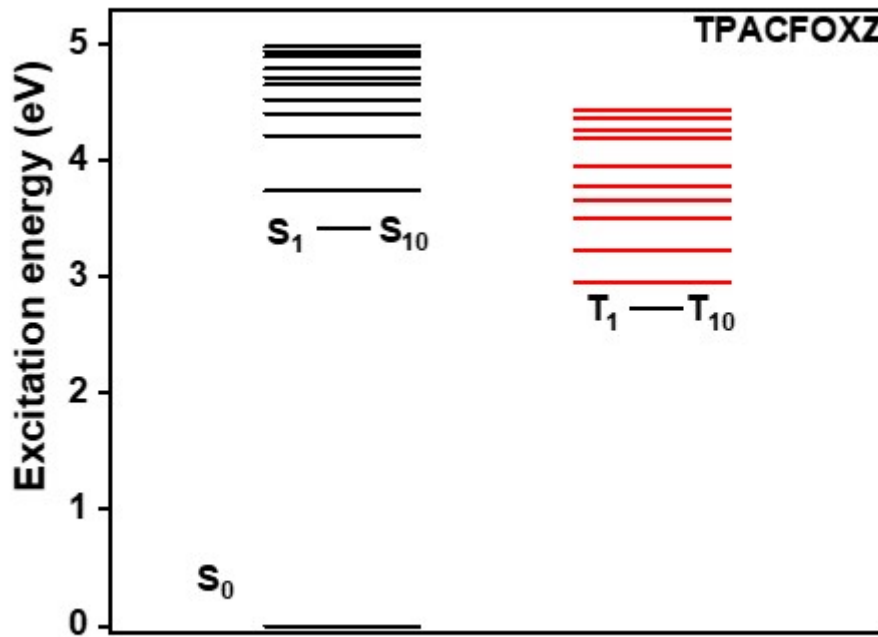


Fig S4. NTO energy level diagram of TPACFOXZ.¹

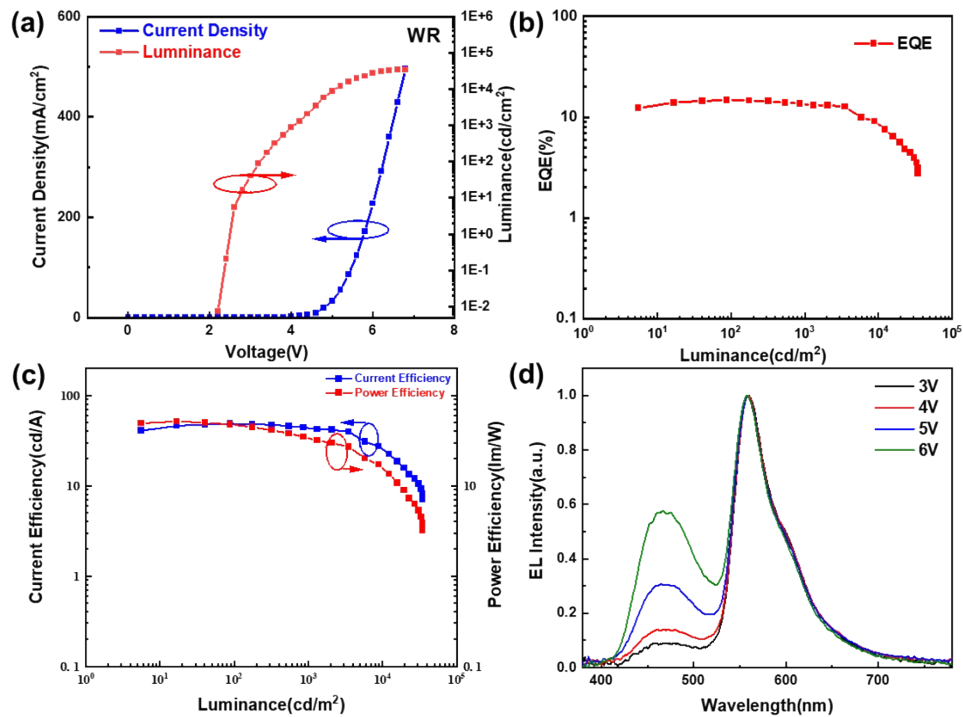


Fig S5. EL performance of the device WR. (a) Current density-voltage-luminance curves. (b) EQE-luminance curve. (c) Current efficiency-luminance-power efficiency curves, (d) EL spectra at different voltages.

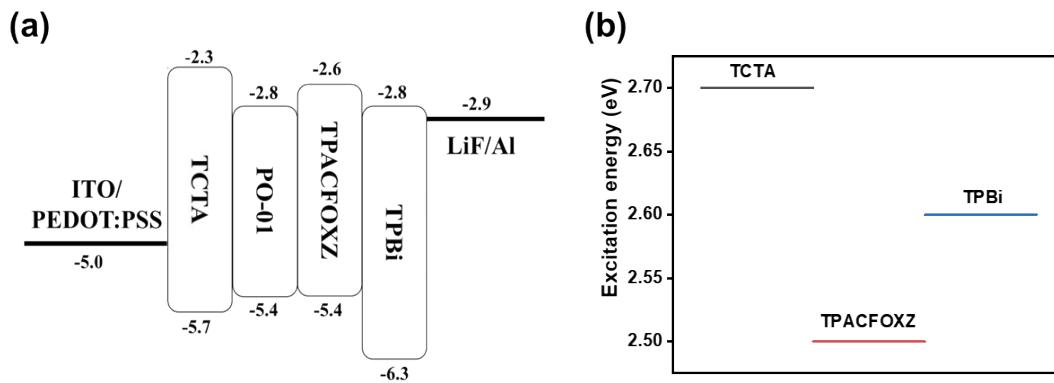


Fig S6. (a) FMO energy level diagram of materials used in W3 (b) T1 energy level diagram of ETL, HTL and EML

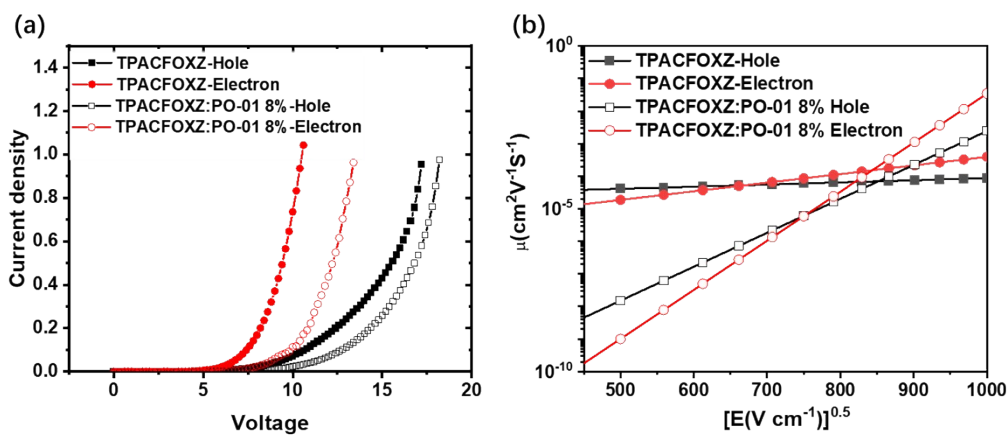


Fig S7. (a) Current density-Voltage curve and (b) Mobility -0.5 power electrical intensity curve of hole-only device ITO/ PEDOT: PSS (40 nm)/ TCTA (20 nm)/ TPACFOXZ or TPACFOXZ: PO-01 (8%) (10 nm)/ TPACFOXZ (15nm)/ TCTA (30 nm)/ Al (100 nm) and electron-only device ITO/ LiF (1 nm)/ TPBi (20nm)/ TPACFOXZ or TPACFOXZ: PO-01 (8%)(10 nm)/ TPACFOXZ (15nm)/ TPBi(30 nm) / LiF (1 nm)/ Al (100 nm)

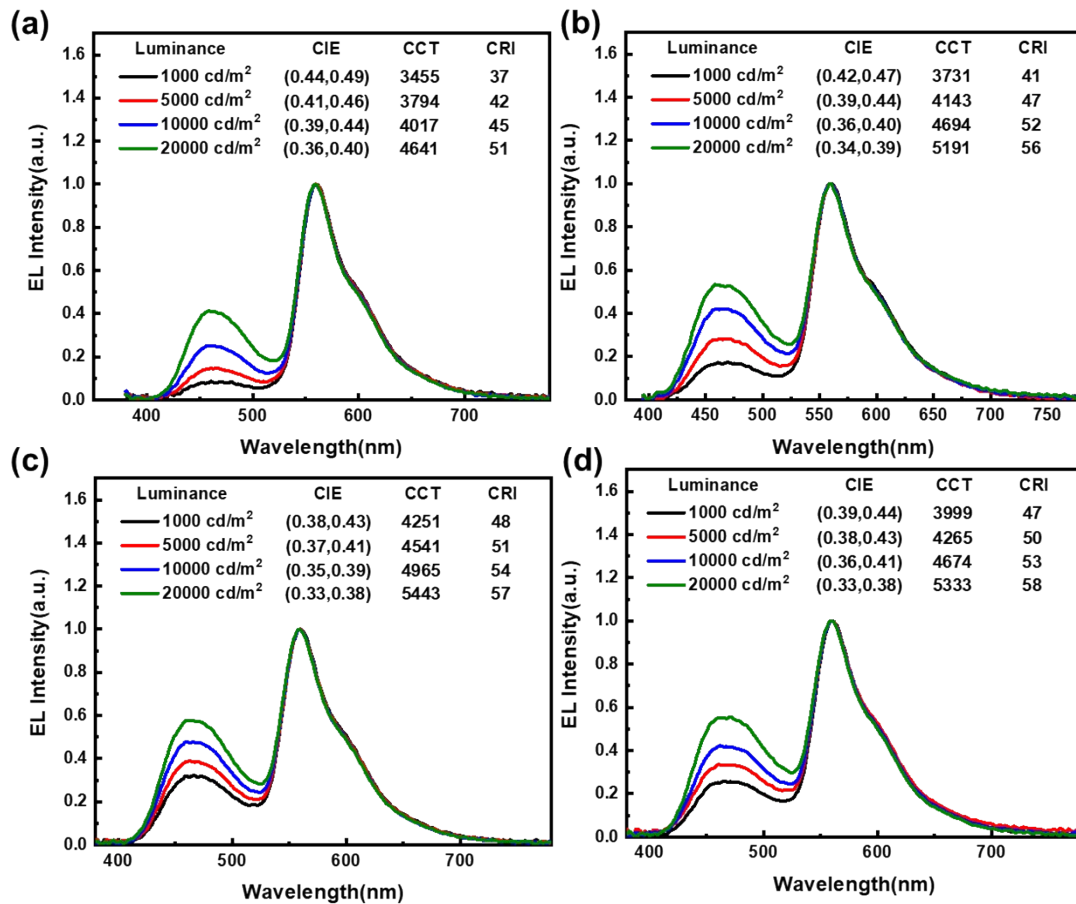


Fig S8. (a), (b), (c), and (d) EL spectra at different luminance of devices **W1**, **W2**, **W3**, and **W4**.

References

- 1 R. Wang, T. Li, C. Liu, M. Xie, H. Zhou, Q. Sun, B. Yang, S. Zhang, S. Xue and W. Yang, Efficient Non-Doped Blue Electro-fluorescence with Boosted and Balanced Carrier Mobilities, *Adv. Funct. Mater.*, 2022, **32**, 2201143.
- 2 H. Zhang, J. Xue, C.L. Li, S. Zhang, B. Yang, Y. Liu, and Y. Wang, Zhang H, Xue J, Li C, Zhang S, Yang B, Liu Y and Y. Wang, Novel Deep-Blue Hybridized Local and Charge-Transfer Host Emitter for High-Quality Fluorescence/Phosphor Hybrid Quasi-White Organic Light-Emitting Diode, *Adv. Funct. Mater.*, 2021, **31**, 2100704.
- 3 X. Wu, J. Zeng, X. Peng, H. Liu, B. Tang and Z. Zhao, Robust sky-blue

aggregation-induced delayed fluorescence materials for high-performance top-emitting OLEDs and single emissive layer white OLEDs, *Chem. Eng. J.*, 2023, **451**, 138919.

4 J. Zhang, J. Sun, Y. Ma, C. Han, D. Ding, Y. Wei and H. Xu, Multiplying Phosphine-Oxide Orientation to Enable Ultralow-Voltage-Driving Simple White Thermally Activated Delayed Fluorescence Diodes with Power Efficiency over 100 lm W⁻¹, *Adv. Funct. Mater.*, 2022, **32**, 2209163.

5 Y. Li, Z. Xu, X. Zhu, B. Chen, Z. Wang, B. Xiao, J. W. Y. Lam, Z. Zhao, D. Ma, and B. Tang, Creation of Efficient Blue Aggregation-Induced Emission Luminogens for High-Performance Nondoped Blue OLEDs and Hybrid White OLEDs, *ACS Appl. Mater. Interfaces*, 2019, **11**, 17592–17601.

6 H. Chen, H. Liu, P. Shen, J. Zeng, R. Jiang, Y. Fu, Z. Zhao, and B. Tang, Efficient Sky-Blue Bipolar Delayed Fluorescence Luminogen for High-Performance Single Emissive Layer WOLEDs, *Adv. Opt. Mater.*, 2021, **9**, 2002019.

7 J. Xu, H. Liu, J. Li, Z. Zhao and B. Tang, Multifunctional Bipolar Materials Serving as Emitters for Efficient Deep-Blue Fluorescent OLEDs and as Hosts for Phosphorescent and White OLEDs, *Adv. Opt. Mater.*, 2021, **9**, 2001840.

8 S. Ying, W. Liu, L. Peng, Y. Dai, D. Yang, X. Qiao, J. Chen, L. Wang and D. Ma, A Promising Multifunctional Deep-Blue Fluorophor for High-Performance Monochromatic and Hybrid White OLEDs with Superior Efficiency/Color Stability and Low Efficiency Roll-Off, *Adv. Opt. Mater.*, 2022, **10**, 2101920.

9 Y. Li, Z. Li, J. Zhang, C. Han, C. Duan and H. Xu, Manipulating Complementarity of Binary White Thermally Activated Delayed Fluorescence Systems for 100% Exciton

Harvesting in OLEDs, *Adv. Funct. Mater.*, 2021, **31**, 2011169.